Temporal and Spatial Regulation of Bone Morphogenetic Protein Signaling in Late Lung Development

Miguel A. Alejandre-Alcázar, Petar D. Shalamanov, Oana V. Amarie, Julia Sevilla-Pérez, Werner Seeger, Oliver Eickelberg, and Rory E. Morty*

Bone morphogenetic proteins (BMPs) play important roles in early lung development. No study to date has addressed a role for BMP signaling in late lung development. We describe changes in the expression and localization of BMP receptors (Bmpr1a, Bmpr1b, and Bmpr2) and Smad (Smad1, Smad4, Smad5, and Smad8) intracellular signaling proteins during the saccular and alveolarization stages of late lung development. BMP signaling, assessed by Smad1/5 phosphorylation, nuclear translocation, and induction of *id1, id2*, and *id3* gene expression, was evident throughout late lung development. Our data indicate that BMP signaling is active during late lung development, and points to roles for the BMP system in septal and vascular development, and in the homeostasis of the epithelial layer of large conducting airways in the mature lung. *Developmental Dynamics 236:2825–2835, 2007.* © 2007 Wiley-Liss, Inc.

Key words: lung development; alveolarization; septation; BMP, bone morphogenetic protein; mouse

Accepted 13 July 2007

INTRODUCTION

The organogenesis of the lung occurs over five separate stages (Roth-Kleiner and Post, 2003; Copland and Post, 2004), during which the surface area available for gas exchange is maximized, and the blood-air barrier is minimized. This is achieved by *branching* of the conducting airways, and subdivision of the developing airspaces into alveoli by a process of *septation* (Roth-Kleiner and Post, 2003; Copland and Post, 2004). Airway *branching* begins in the embryonic stage [4–7 weeks post conception in humans, embryonic days (E) 9.5–12 in mice], and continues through the pseudoglandular (5–17 weeks in humans, E12–E16.5 in mice) and canalicular (16–26 weeks in humans, E16.5–E17.5 in mice) stages, constituting the stages of early lung development. During late lung development, the distal airways form saccular units in the saccular stage [24–38 weeks in humans, E17.5- postnatal day (P) 4]. Secondary septae then divide these units (*septation*) during the alveolar stage (36 weeks pre-term to 36 months post-natal in humans, P4-P28 in mice), forming mature alveoli. This sequence of events is carefully controlled by the concerted action of transcription factors, mechanical forces, and growth factors (Warburton et al., 2000; Cardoso, 2001; Jankov and Tanswell, 2004). Amongst the growth factors, members of the bone morphogenetic protein (BMP) family have been implicated in lung branching. However, their role, if any, has not been addressed in late lung development (Jankov and Tanswell, 2004; Roth-Kleiner and Post, 2005).

The BMPs, which belong to the transforming growth factor (TGF)-β superfamily of polypeptide growth factors, have been ascribed numerous roles in vertebrate development, including cell differentiation, migration, proliferation, and apoptosis (Miya-

Department of Internal Medicine, University of Giessen Lung Center, Justus Liebig University, Giessen, Germany
Grant Sponsor: Deutsche Forschungsgemeinschaft; Grant number: SFB547 “Cardiopulmonary Circulation”; Grant Sponsor: The “Excellence Cluster Cardiopulmonary System” of the Universities of Giessen and Frankfurt and the Max-Planck-Institute for Heart and Lung Research; Grant Sponsor: The European Commission Sixth European Framework Programme “Pulmotension.”
***Correspondence to: Rory E. Morty, Department of Internal Medicine, University of Giessen Lung Center, Justus Liebig University, Aulweg 123 (Raum 6-11), D-35392 Giessen, Germany. E-mail: rory.morty@innere.med.uni-giessen.de**

DOI 10.1002/dvdy.21293
Published online 5 September 2007 in Wiley InterScience (www.interscience.wiley.com).

zono et al., 2005). The BMP family of ligands currently numbers over 22 members (de Caestecker, 2004). These ligands bind to their cognate type I receptors Bmpr1a [also called activin-like kinase (ALK)-3] or Bmpr1b (also called ALK6), which subsequently activate the type II receptor (Bmpr2), thereby initiating a signaling cascade primarily via second-messenger Smad proteins, namely Smads 1, 4, and 5 (Miyazono et al., 2005).

Several lines of evidence have implicated BMPs in early lung development (Dewulf et al., 1995; Weaver et al., 1999; Warburton et al., 2005). The BMP-4 ligand is expressed at the developing tips of the distal endoderm and in the adjacent mesenchyme of the developing lung (Bellusci et al., 1996). Addition of exogenous BMP-4 to embryonic lung explants stimulated lung branching in vitro (Bragg et al., 2001; Shi et al., 2001), and misexpression of BMP-4 throughout the distal lung epithelium impaired lung growth, distended the terminal buds, and caused airspace enlargement (Bellusci et al., 1996). Furthermore, the BMP antagonist gremlin regulates proximal-distal patterning of the lung (Lu et al., 2001), and antisense knockdown of Smad1, a key intracellular transducer of BMP signals, and overexpression of Smurf1, which promotes ubiquitination-dependent degradation of Smad1 and Smad 5, both negatively regulated lung branching (Shi et al., 2004; Chen et al., 2005). However, BMP-4 expression declines prior to the saccular stage, and it has been suggested that this indicates that BMP signaling is not required for late lung development (Roth-Kleiner and Post, 2005).

Recent reports that BMP ligands regulate myocyte differentiation of lung fibroblasts (Jeffery et al., 2005a), collagen production by mouse pulmonary myofibroblasts (Buckley et al., 2004), and cell senescence in alveolar epithelial cells (Izumi et al., 2006), together with the observation that Bmpr1a regulates the proliferation, survival, and morphogenic behavior of distal lung epithelial cells (Eblaghie et al., 2006), suggested to us that the BMP signaling system may also be active in late lung development. In this study, we have clarified the isoform expression of Bmpr1a in the developing mouse lung, and we document that changes in the expression and activity of the BMP signaling machinery do occur during late lung development. These data provide the first evidence that BMP signaling is active during late lung development.

RESULTS AND DISCUSSION

One of the hallmarks of late lung development is the division of the saccular airspaces by the formation of secondary septae from the primary septae, a process that forms mature alveoli. Thus, a progressive decrease in the size of the alveolar airspaces together with a concomitant increase in the total number of alveoli is a key feature of late lung development. This phenomenon is illustrated in Figure 1A and B. In the insets in Figure 1A and B, an area of a lung from a mouse at post-natal day P7 (Fig. 1A) is compared with a similarly sized area of a lung from a mouse at day P28 (Fig. 1B). It is evident from these two insets that the septal wall thickness is decreased while the number of alveolar airspaces per unit lung area increases as the lung develops over this period. This development of the alveolar airspaces was accompanied by changes in the expression of mRNA encoding both BMP receptors and BMP-responsive Smad proteins (Fig. 1C, quantified in Fig. 1D). While the levels of *bmpr1a* and *bmpr1b* mRNA did not change significantly (Fig. 1D), a significant increase in *bmpr2* expression was evident in both the saccular (E17 to E19) and alveolar (P7 to P14) stages. Similarly, while *smad1* and *smad4* mRNA levels decreased significantly in the alveolar stage (Fig. 1D), *smad5* levels remained unchanged. In contrast, *smad8* mRNA levels increased significantly in the saccular and alveolar stages (Fig. 1D). These data thus suggested that in addition to previously described changes in BMP signaling during the branching stages of early lung development, BMP signaling was also regulated during late lung development.

The type I BMP receptor Bmpr1a is emerging as an important mediator of proliferation, survival, and morphogenetic behavior of distal lung epithelial cells, and hence, perhaps late lung development (Eblaghie et al., 2006). Two different *bmpr1a* mRNA splice-isoforms have been described: a long *bmpr1a* splice-isoform (GenBank™ accession number NM_009758.1; Fig. 2A), and a shorter version, called BRK-1 (Koenig et al., 1994; GenBank™ accession number U04672; Fig. 2A), which lacks an 89-bp insertion present in the long splice-isoform (described schematically in Fig. 2E). No data are currently available concerning the functional consequences of preferential or exclusive expression of one splice-isoform over the other. Paradoxically, the long *bmpr1a* splice-isoform encodes a shorter protein (Fig. 2B), due to the presence of a stop-codon in the 89-bp insertion (see Fig. 2E). We were unable to amplify the long *bmpr1a* splice-isoform from total mRNA isolated from the mouse lung (Fig. 2C; lane F1+R1). However, partial sequences common to both splice-isoforms were amplified with primer combinations F1+R2 and F1+R3 (Fig. 2C). Using *bmpr1a* primers F1 and R4 (indicated in Fig. 2E), a 1,599-bp open-reading frame was amplified from whole lung mRNA that lacked the 89-bp insertion evident in the long *bmpr1a* splice-isoform. This sequence has been deposited in the GenBank™ database under accession number AY365062. While this *bmpr1a* mRNA was the only *bmpr1a* mRNA species detected in the mouse lung and heart (Fig. 2C), we were able to detect sequences corresponding to the 89-bp fragment when using mouse genomic DNA as a template (Fig. 2D; lane 1), but not when using mouse lung cDNA (Fig. 2D; lane 2). In contrast, amplicons were generated when using primers F2+R2 with both mouse genomic (Fig. 2D; lane 3) and mouse lung cDNA (Fig. 2D; lane 4), and the difference in size between the two amplicons corresponded to a stretch of sequence of approximately 100 bp (Fig. 2D). These data suggest that the 89-bp sequence represents part of the intronic structure of the *bmpr1a* gene.

Immunoblot analysis of whole lung extracts from developing mouse lungs supported the PCR data illustrated in Figure 1, and demonstrated changes in the expression of BMP receptors and Smad proteins during late lung development (Fig. 3A; quantified in Fig. 3B). Bmpr1 expression was tran-

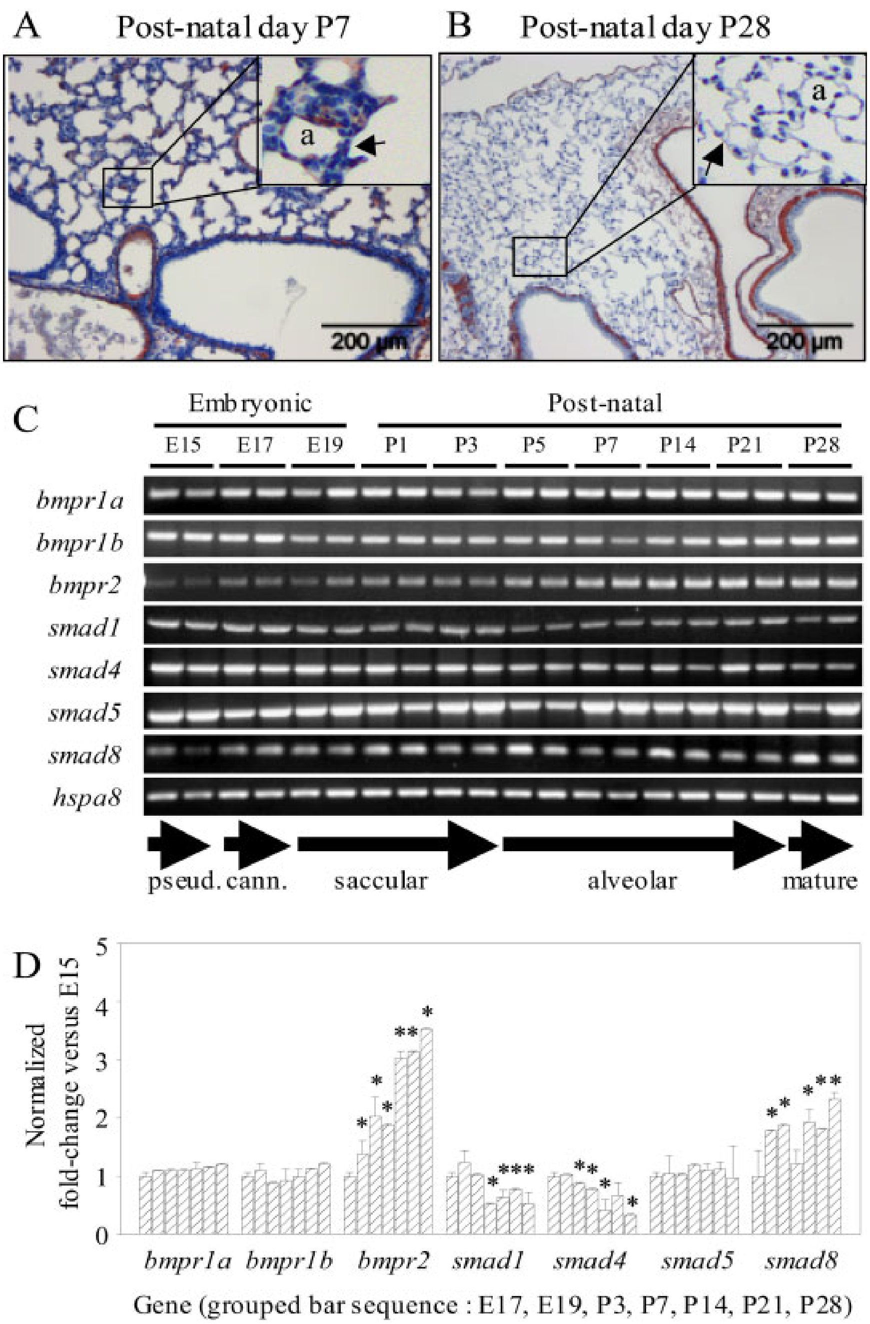

Fig. 1. Expression of the BMP signaling machinery during the late lung development. An increase in the number of alveolar air-spaces (an example of which is denoted by "a") and a decrease in the thickness of septal walls (indicated with an arrow) are evident between day P7 (**A**) and day P28 (**B**) in the developing mouse lung. Representative sections from the lungs of mice at post-natal days P7 and P28 were stained for smooth muscle actin (to reveal muscularized structures, including large airways and vessels) and counter-stained with hematoxylin, to stain basophilic structures, including cell nuclei. **C:** Changes in the expression of genes, assessed by RT-PCR, encoding the BMP signaling machinery were observed in the saccular (E17.5-P4) and alveolar (P4-P28) stages of late lung development in mice. Amplicons illustrate samples from two different mouse lungs per developmental stage that are representative of trends observed in at least six other mouse lungs at the same developmental stage. **D:** For quantification of changes in mRNA expression, amplicon bands derived from six different mouse lungs were selected for densitometric analysis. Band intensities from specific samples were normalized for loading using the *hspa8* band from the same sample. Changes are expressed relative to the *hspa8*-normalized pixel density (PD) of the E15 sample: [band PD/*hspa8* band PD]/[band PD (E15)/*hspa8* band PD (E15)]. Data reflect the mean normalized fold-change versus E15 $\pm$ S.D. (n = 6). $^*P < 0.05$. Pseud., pseudoglandular; can., canalicular.

siently but significantly two-fold increased in the saccular stage, but by post-natal day P28 fell to levels significantly (approximately 50%) lower than those observed at embryonic day E15 (Fig. 3A and B). Bmpr1b protein levels were significantly downregulated by post-natal day P28 to less than 10% of their expression levels at embryonic day E15 (Fig. 3A and B). Conversely, a gradual and significant increase in Bmpr2 expression was evident during the alveolar stage (post-natal days P7 to P28). These observations are interesting, since Bmpr1a and Bmpr1b generally promote opposing functions, where signaling via Bmpr1a promotes cell proliferation, while signaling via Bmpr1b is antiproliferative, promoting mitotic arrest and apoptosis (Panchision et al., 2001). Given the transiently increased (post-natal days P3 and P7) and then slightly (but significantly) decreased (post-natal days P14 to P28) expression levels of Bmpr1a, and the consistently and strongly reduced (post-natal days P14 to 28) expression of Bmpr1b over the time-course of our study, data we describe here suggest that Bmpr1a-directed signaling is favored as normal, late lung development proceeds. Supporting this idea, the Bmpr1a-Bmpr1b expression balance is reversed in experimental models of arrested late lung development, for example, in a hyperoxia model of bronchopulmonary dysplasia, a disorder characterized by pronounced alveolar hypoplasia and arrested late lung development, where Bmpr1b expression is favored over that of Bmpr1a (Alejandre-Alcázar et al., 2007). These data would suggest that the pro-proliferative activity of BMP signaling is maintained in the normal, developing mouse lung by maintaining high levels of Bmpr1a expression.

The significant increase in the expression levels of Bmpr2 (Fig. 3) is also noteworthy. The transduction of BMP signals is facilitated by complex formation between type I and type II BMP receptors. Levels of Bmpr2 regulate the stoichiometry of these complexes (Yu et al., 2005). Changes in the heteromeric BMP receptor complex stoichiometry impact BMP signaling, and can shift the balance from a growth inhibitory to a mitogenic response (Frank et al., 2005). In the absence of Bmpr2, type I receptors can form atypical complexes with other type I and II receptors, for example, the type I activin A receptor (Acvr1) and the activin receptor IIa (Acvr2a) (Yu et al., 2005). These atypical complexes do not form in the presence of Bmpr2, and exhibit peculiar BMP signaling (Yu et al., 2005). The relative expression levels of different BMP receptors may also alter the density of pre-formed versus ligand-induced receptor complexes at the cell surface, which direct different BMP signaling pathways (Hassel et al., 2003). Thus, the significant increase in Bmpr2 expression may also serve to direct the outcome of BMP signaling during late lung development. Changes in the expression levels of Smad proteins were also observed during late lung development (Fig. 3). Both Smad1 and Smad4 protein levels significantly decreased, exhibiting expression levels at post-natal day P28 that were less then 10% of the expression levels at embryonic day E15. In contrast, both Smad5 and Smad8 protein levels significantly increased by as much as three-fold by post-natal day P28 (Fig. 3A and B). These data would suggest that Smad1 signaling is dampened, while Smad5 and Smad8 signaling is promoted, during late lung development.

Dramatic changes in the cellular localization of BMP receptors (Fig. 4) were evident during late lung development. Pronounced staining for both Bmpr1a (Fig. 4A) and Bmpr1b (Fig. 4C) was evident in the alveolar septae during early lung development (stage P7, at the start of the alveolarization stage), although no staining was evident in either the vasculature or the large airway epithelium. In contrast, at stage P28, at the end of the alveolarization stage, substantially reduced staining was evident for Bmpr1a in the alveolar septae (although it was still detected in type II pneumocytes, typically present at the corners of the alveoli; Fig. 4B, arrows) and pronounced staining was now also evident in the airway epithelium (Fig. 4B). Similarly, no staining was detected for Bmpr1b in the alveolar septae, although some staining was evident in the large airway epithelium (Fig. 4D). These data indicate a spatial change in the expression of type I

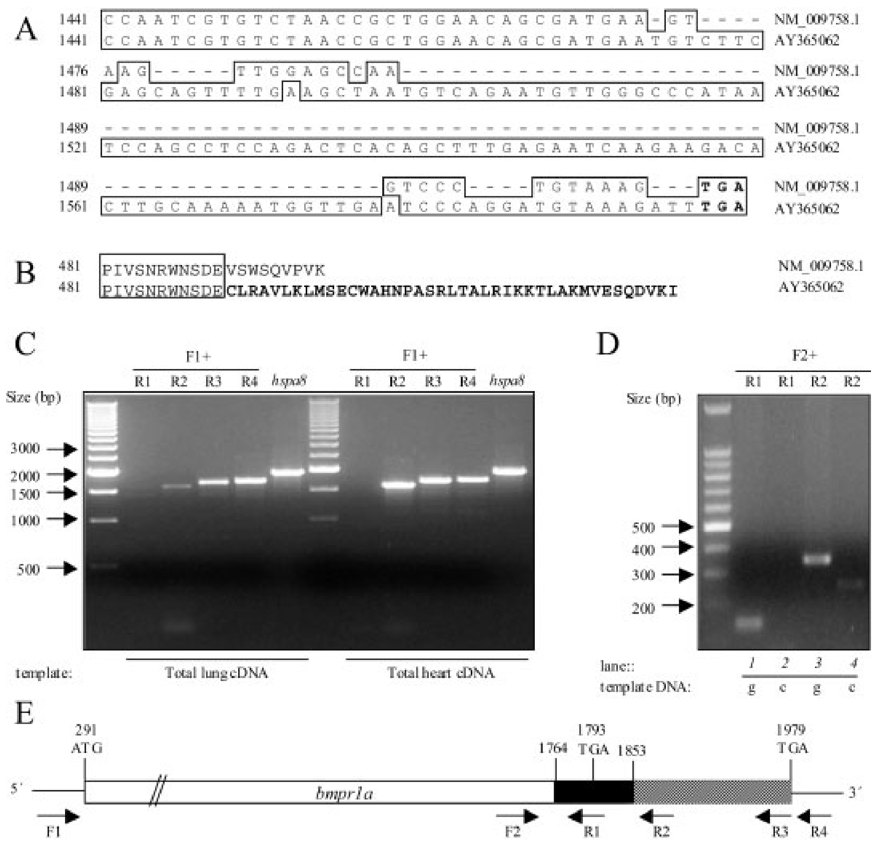

Fig. 2. The short *bmpr1a* splice-isoform is expressed in the lungs of mice during late lung development. **A:** Comparison of the 3′ end of the primary nucleotide sequences of the long (GenBank™ accession number NM_009758.1) and short (GenBank™ accession number AY365062) *bmpr1a* isoforms. **B:** Comparison of the deduced amino acid sequences of the C-termini of the mature Bmpr1a polypeptides encoded by the long (GenBank™ accession number NM_009758.1) and short (GenBank™ accession number AY365062) *bmpr1a* splice-isoforms. **C:** Exclusive detection of the short *bmpr1a* splice-isoform in the lung and heart of mice at stage P28. PCR amplicons were generated from RNA isolated from the lung and heart of mice at stage P28, using the primer combinations depicted in the schematic in E. Expression of the *hspa8* gene served as a loading control. Primer combination F2+R1 would exclusively detect the long *bmpr1a* isoform. **D:** An amplicon encoding part of the *bmpr1a* long splice-isoform can be generated from mouse genomic DNA (g) but not mouse lung cDNA (c) templates. **E:** Schematic illustration of the *bmpr1a* mRNA, displaying characteristics of both the long and short splice-isoforms. The long splice-isoform contains an 89-bp insertion (indicated by the black box) that contains a stop-codon at position 1,793. The short splice-isoform (in which the region illustrated in black is missing) thus contains a longer, additional stretch of coding sequence (indicated by the shaded box), until the stop-codon at position 1,979 is reached. Although the long splice-isoform contains both the region indicated in black and the region indicated by shading, a premature stop-codon is reached at position 1,793. Therefore, the long splice-isoform expresses a shorter polypeptide (as is evident in B).

BMP receptors during late lung development, and also support the trends observed in the immunoblot data (Fig. 3), where reduced levels of Bmpr1b expression were observed as late lung development progressed. Staining for Bmpr2 at post-natal stage P7 was observed in the alveolar septae (Fig. 4E), in the vascular smooth muscle, and most notably, in the endothelial lining of the developing lung (Fig. 4E, inset). This expression is consistent with the proposed essential roles for Bmpr2, and, indeed, BMP signaling, in vasculogenesis (Jeffery et al., 2005b). By stage P28, although faint staining was still evident in the vessels (Fig. 4F, inset) and in some type II pneumocytes, more pronounced staining was now also evident in the airway epithelium (Fig. 4F). The dramatically increased expression of all three BMP receptors in the epithelial lining of large airways at the end of the alveolarization stage hints at a previously unrecognized role for BMP signaling

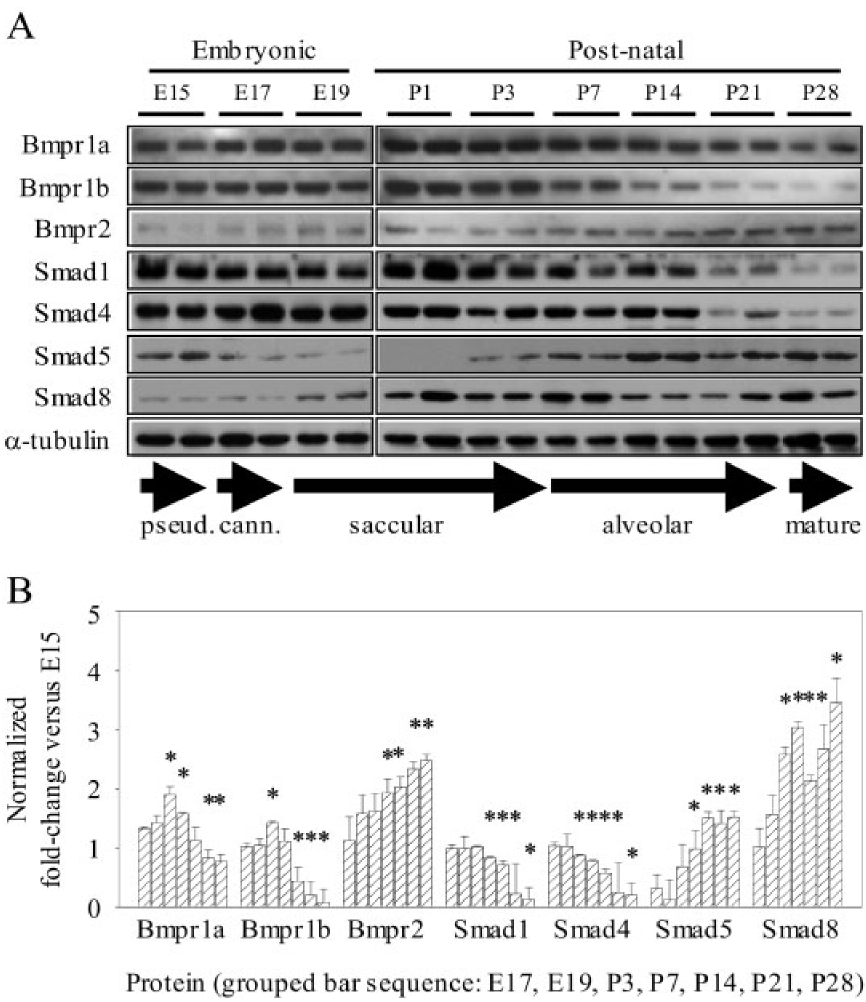

Fig. 3. Changes in the protein expression of the BMP signaling machinery, assessed by immunoblot, were observed in the saccular (E17.5-P4) and alveolar (P4-P28) stages of late lung development in mice (**A**). Blots illustrate 10-μg samples from two different mouse lungs per developmental stage that are representative of trends observed in at least six other mouse lungs at the same developmental stage. **B:** Bands derived from six different mouse lungs were selected for densitometric analysis. Band intensities from samples were normalized for loading using the α-tubulin band from the same sample. Expression ratios for immunoblot data reflect values normalized for tubulin: [band PD/tubulin band PD]/[band PD (E15)/tubulin band PD (E15)]. Data reflect the mean normalized fold-change versus E15 $\pm$ S.D. ($n = 6$). **P* < 0.05. Pseud., pseudoglandular; can., canalicular.

in the homeostasis of the airway epithelium in the developed lung. This idea is supported by the suggestion that BMP activity in the bronchial epithelium may play a role in airway inflammation in allergic asthma (Rosendahl et al., 2002).

Dramatic changes in the localization of Smad proteins were also evident during late lung development (Fig. 5). Smad1 protein expression was evident throughout the developing alveolar airspaces and the vessel walls at stage P7 (Fig. 5A). Staining was pronounced in the endothelium and the underlying smooth muscle layer of the developing vessels (Fig. 5C). The nuclear staining pattern was strongly indicative of an activated (thus phosphorylated) Smad1. Interestingly, no Smad1 staining was evident in the airway epithelium (Fig. 5E), although some staining was evident in the underlying airway smooth muscle layer. In contrast, by stage P28, staining for Smad1, while still evident in the endothelial layer of small vessels and the airway smooth muscle (Fig. 5F), was dramatically increased in the large airway epithelium (Fig. 5B). At stage P28, Smad1 staining was apparent in both the nuclear (indicating activated, phosphorylated Smad1) as well as the cytosolic compartment (indicating inactive, non-phosphorylated Smad1; Fig. 5F). Both nuclear and cytosolic staining were detected for Smad1 in type II pneumocytes in the alveolar airspaces, although no staining was detected in the more elongate, thinner, type I pneumocytes (Fig. 5G, arrows). Staining for Smad4 at stage P7 was also evident in the endothelial and smooth muscle layers of the developing vessels, as well as in the airway epithelial cells and underlying smooth muscle, and the alveolar septae (Fig. 5H). The nuclear localization of the staining in every case indicated that the Smad4 signaling pathways were largely active. By stage P28, Smad4 staining was generally reduced (consistent with the immunoblot data in Fig. 3). However, staining remained evident in type II pneumocytes, but not type I pneumocytes, as well as in endothelial cells and the airway epithelium (Fig. 5I). As with Smad1 at stage P28, both cytosolic and nuclear pools of Smad4 were evident, suggesting that the level of Smad4-mediated signaling was less at stage P28 (late alveolarization stage) than it was at P7 (at the start of the alveolarization stage).

In contrast to Smad1 and Smad4 (Fig. 4), the localization of Smad5 and Smad8 did not change over the course of late lung development (Fig. 6). Smad5 staining was apparent in the cytosol of interstitial epithelial cells, and in the walls of the pulmonary vessels at post-natal stage P7 (Fig. 5A). A similar pattern was observed at post-natal stage P28 (Fig. 5B), although some nuclear staining was also observed, suggesting activation of Smad5 at post-natal stage P28. Similarly, Smad8 remained localized to the cytosol of interstitial epithelial cells, and in the walls of the pulmonary vessels at post-natal stages P7 (Fig. 6C) and P28 (Fig. 6D), with no nuclear localization evident at either stage. Thus, both Smad1 and Smad4 (Fig. 5), but not Smad5 and Smad8 (Fig. 6), exhibited dramatic changes in spatial localization during late lung development.

Together, these data demonstrate a dramatic shift in the expression and localization of BMP receptors and

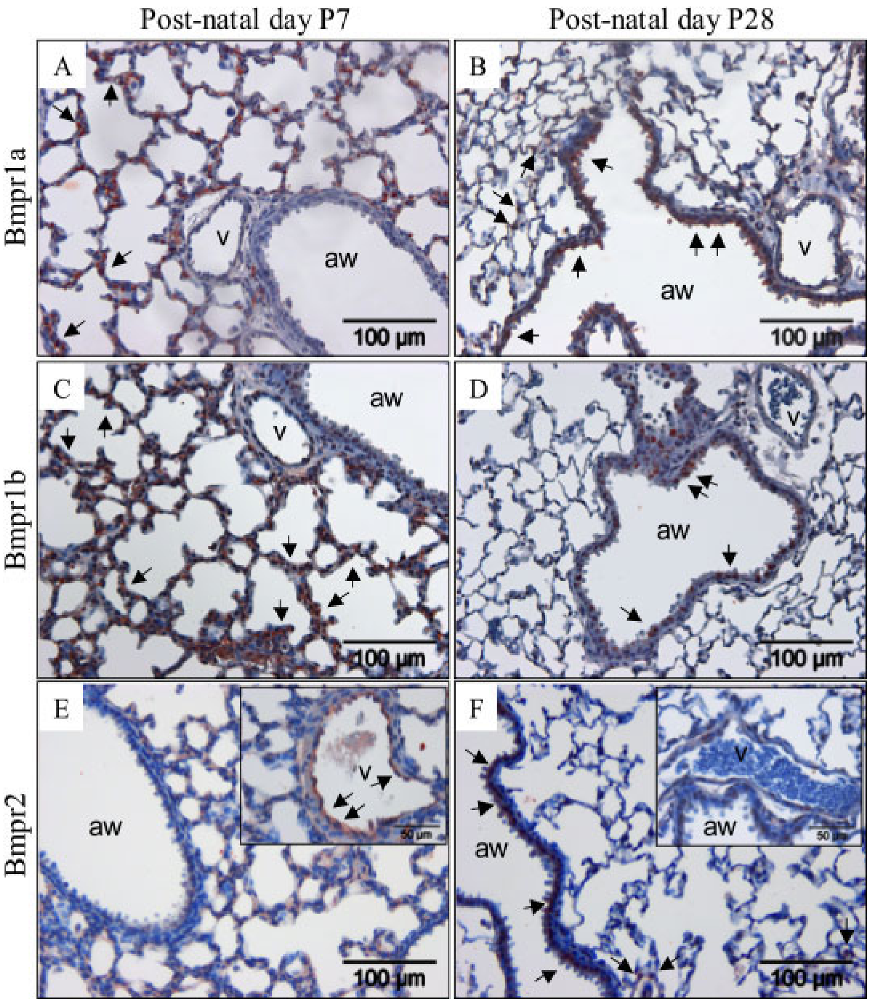

Fig. 4. Temporal and spatial changes in BMP receptor expression occur during late lung development. BMP receptor expression was localized in the lungs of mice at stage P7 (left-hand column; panels **A,C,E**) and P28 (right-hand column; panels **B,D,F**) by immunohistochemical staining. Insets in E and F, which are not taken from areas within the panels, indicate magnified views of vessel wall staining. The areas illustrated are representative of staining patterns observed in three separate animals per developmental stage. aw, airway; v, vessel. Arrows indicate examples of stained cells.

Smads between post-natal stages P7 and P28. All BMP receptors and Smads were expressed in the developing alveoli at post-natal stage P7, including nuclear-localized (and thus active) Smad1 and Smad4 (Figs. 5 and 6), suggesting very active Smad signaling in this tissue, although Smad1 was not detected in the airway epithelium. By post-natal stage P28. the presence of Smad1 and Smad4 in the lung interstitium was reduced, although it became more pronounced in the epithelium lining large conducting airways (Fig. 5). Furthermore, while absent in the large airway epithelium at post-natal stage P7, Bmpr1a and Bmpr2 staining was evident in the large airway epithelium at post-natal stage P28 (Fig. 4). We propose that this shift in expression levels and localization of BMP receptors and Smad proteins may serve to focus BMP signaling in specific areas of the lung at specific stages of lung development. It should also be noted that BMP ligands can signal via Smad-independent pathways involving mitogen-activated protein (MAP) kinases (Miyazono et al., 2005; Yang et al., 2007). The relative impact of our observations on BMP-induced MAP kinase signaling has not been assessed in this study.

To assess whether BMP signaling was indeed active throughout late lung development, we employed both a direct and indirect measure of BMP signaling activity. Both Smad1 and Smad5 are phosphorylated in response to BMP stimulation (Miyazono et al., 2005). Smad1 phosphorylation was detected in the pseudoglandular, canalicular, and saccular stages of lung development (Fig. 7A and D). At the end of the alveolar stage of lung development (between day P21 and P28), a shift in the phosphorylation of Smad proteins was observed, where reduced Smad1 phosphorylation, but increased Smad5 phosphorylation, were evident (Fig. 7A, B, and D). This shift coincided with the end of late lung development. These data are consistent with the decreased expression of Smad1 protein, and increased expression of Smad5 protein, during late lung development (Fig. 3).

Expression of the BMP-responsive genes *id1, id2*, and *id3*, which encode small helix-loop-helix "inhibitor of differentiation" proteins, are popularly used read-outs of BMP signaling (Miyazono and Miyazawa, 2002). The expression of *id1, id2*, and *id3* was assessed by semi-quantitative RT-PCR (Fig. 7C and E). A significant increase in the expression of mRNA encoding all three Id proteins was observed over the course of late lung development, indicating that the BMP signaling system was indeed active. In the case of *id1* and *id3*, expression remained significantly elevated (relative to E15 levels) even into stage P28. However, after a transient and significant increase, expression of *id2* dropped significantly, and by stage P28 had returned to levels comparable to those observed at E15 (Fig. 7C and E). These data provide both direct and indirect evidence that BMP signaling was active over the course of late lung development.

Signaling by the BMP family of growth factors has been implicated in various phases of early lung development, particularly in branching morphogenesis of the lung (Dewulf et al., 1995; Weaver et al., 1999; Warburton et al., 2005). However, BMP-4 expression declines prior to the saccular stage, and it has therefore been suggested that BMP signaling is not required for late lung development (Roth-Kleiner and Post, 2005). We present data in this study indicating that the BMP signaling system is indeed active during late lung development. This idea is supported by the

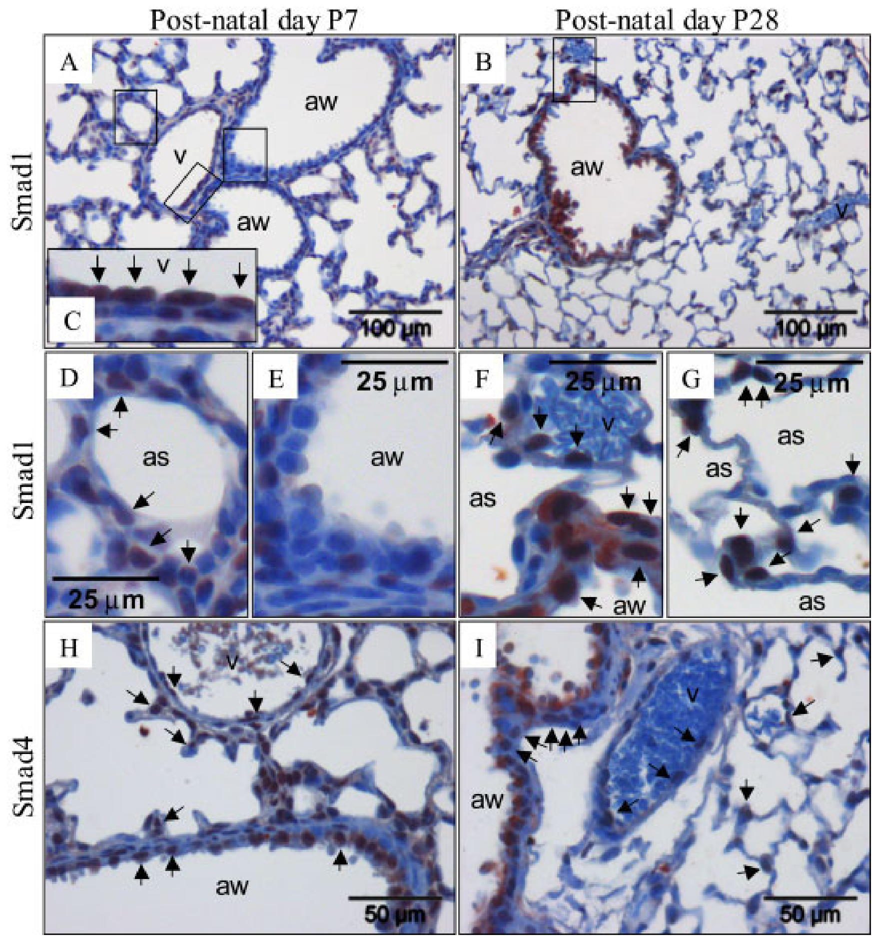

Fig. 5.

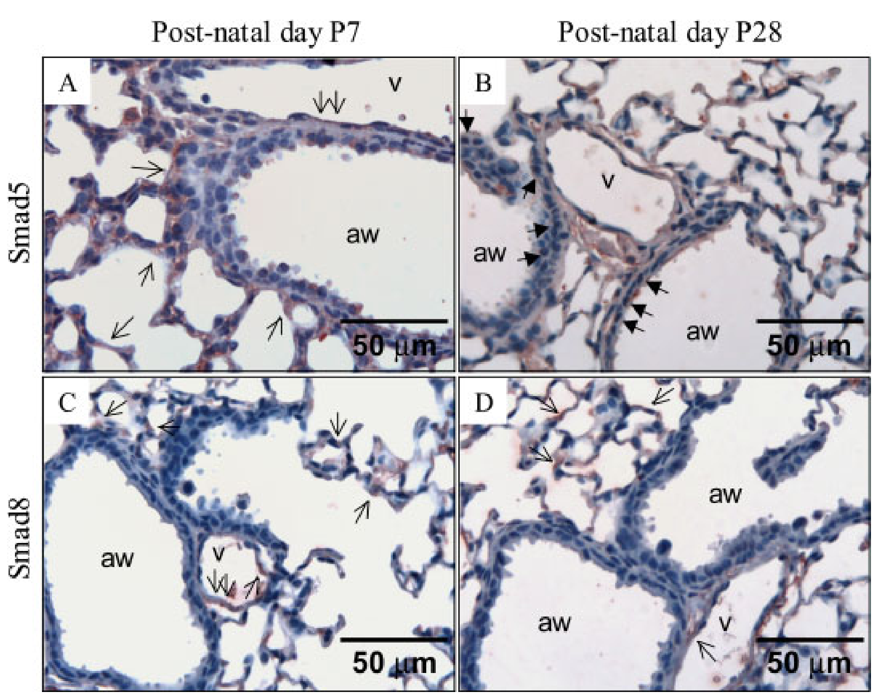

Fig. 6.

Fig. 5. Temporal and spatial changes in BMP-responsive Smad1 and Smad4 protein expression occur during late lung development. Smad expression was localized in the lungs of mice at stage P7 (left-hand column) and P28 (right-hand column) by immunohistochemical staining. **A–G:** Smad1. C–E indicate magnified areas from a P7 lung, while insets in F and G indicate magnified areas from a P28 lung. When an inset has been derived from A or B, this is indicated by a black box in the respective panel. **H,I:** Smad4. The areas illustrated are representative of staining patterns observed in three separate animals per developmental stage. as, alveolar airspaces; aw, airway; v, vessel. Arrows indicate examples of stained cells.

Fig. 6. Localization of BMP-responsive Smad5 and Smad8 proteins during late lung development. Smad expression was localized in the lungs of mice at stage P7 (left-hand column) and P28 (right-hand column) by immunohistochemical staining. **A,B:** Smad5. **C,D:** Smad8. aw, airway; v, vessel. The areas illustrated are representative of staining patterns observed in three separate animals per developmental stage. Arrows with open arrowheads indicate areas of diffuse staining, while arrows with closed arrowheads indicate nuclear staining for Smad5.

finding that some BMP ligands, for example BMP-6, can be detected in the adult mouse lung (Wall et al., 1993), and that *bmp3*$^{-/-}$ null mice develop lung abnormalities perinatally on a C57Bl/6 inbred background (Eblaghie et al., 2006). The temporal and spatial changes that we describe both in BMP receptor expression, as well as in Smad protein expression and activation, suggest that BMP signaling plays an important and specific role in directing various aspects of late lung development. Expression of both Bmpr1a and Bmpr1b appears to be important for septal development during the saccular and early alveolarization stages, an idea supported by the findings that Bmpr1a can regulate the proliferation and survival of distal lung epithelial cells (Eblaghie et al., 2006) and that BMP signaling via *id2* modulates the production of extracellular matrix by lung myofibroblasts (Izumi et al., 2006). Additionally, Bmpr2 appears to be particularly active in vascular development. The aberrant pulmonary vascular homeostasis associated with defective expression or function of Bmpr1a and Bmpr2 lend credence to this idea (Trembath et al., 2001; Du et al.,

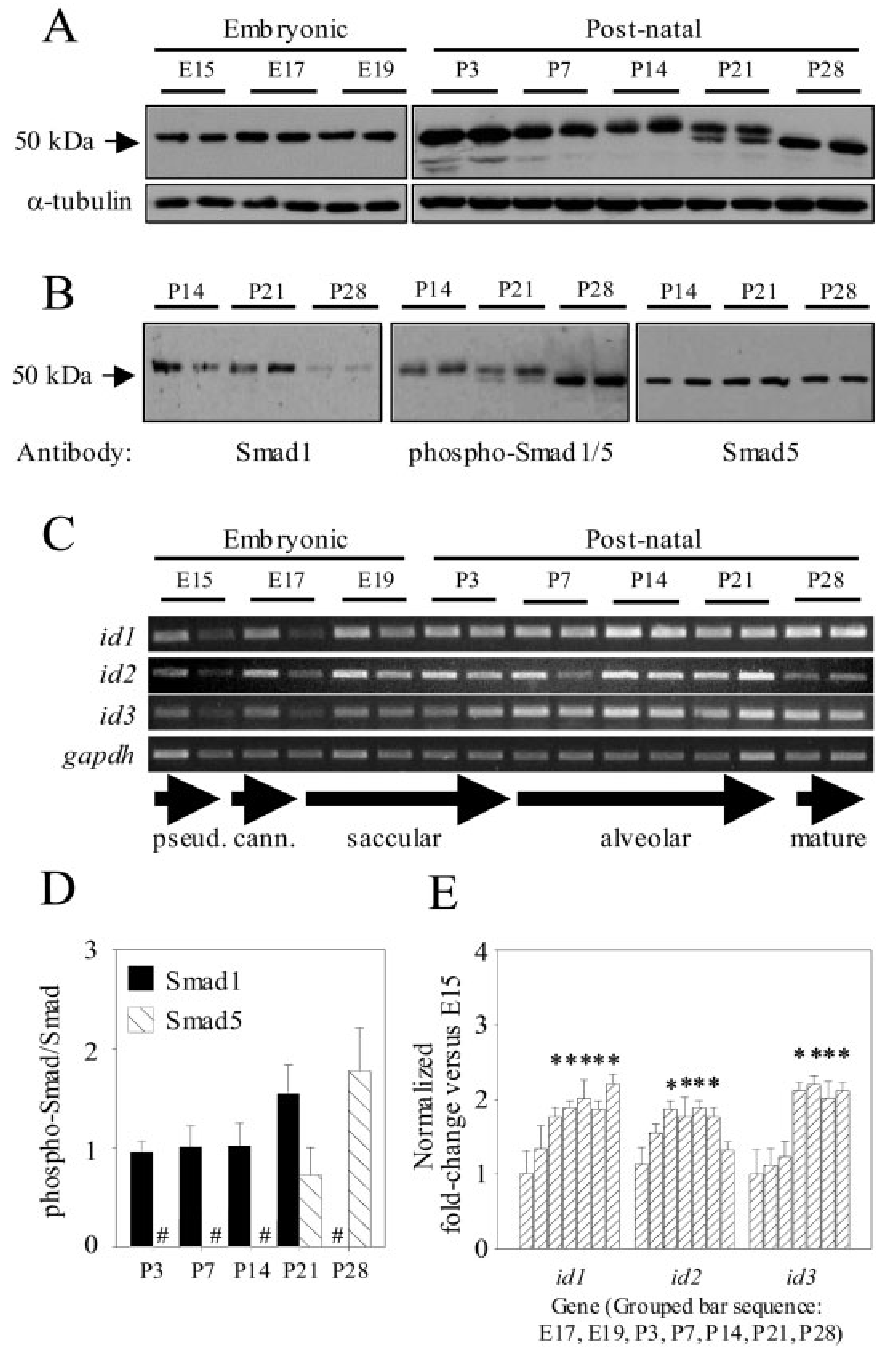

Fig. 7. Direct and indirect assessment of BMP signaling during late lung development. **A:** Smad1/5 phosphorylation as assessed by immunoblot in protein extracts from lungs from mice during the saccular (E17.5-P4) and alveolar (P4-P28) stages of late lung development. The total Smad1 and Smad5 panels are available in Figure 3, while a α-tubulin loading control is indicated in the α-tubulin blot. These data are quantified in D. **B:** To support the idea of a class-switch from Smad1 to Smad5 phosphorylation, duplicate proteins samples from lungs at post-natal stages P14, P21, and P28 were loaded as three separate sets onto the same gel, and blotted to the same membrane. The three sets were separately incubated with anti-Smad1, anti-phospho-Smad1/5, and anti-Smad5. After development, the blots were re-assembled to facilitate comparison of the sizes of the Smad1, Smad5, and phospho-Smad1/5 bands. **C:** Expression of the BMP-inducible target genes *id1, id2*, and *id3* are illustrated during the saccular (E17.5-P4) and alveolar (P4-P28) stages of late lung development. The expression of the *gapdh* gene served as a loading control. Amplicons illustrate samples from two different mouse lungs per developmental stage that are representative of trends observed in at least six other mouse lungs at the same developmental stage. These data are quantified in E. **D:** The phospho-Smad bands in A and the total Smad bands in Figure 3A derive from the same samples. Phospho-Smad bands and total Smad bands derived from four different mouse lungs were selected for densitometric analysis. Band intensities from each sample were normalized for loading using the α-tubulin band from the same sample. Expression ratios for immunoblot data reflect values normalized for tubulin: [phospho-Smad band PD/tubulin band PD]/[Smad band PD/tubulin band PD]. Data reflect the mean normalized fold-change versus E15 ± S.D. (n = 4). **E:** For quantification of changes in *id* mRNA expression, amplicon bands derived from six different mouse lungs were selected for densitometric analysis. Band intensities from specific samples were normalized for loading using the *hspa8* band from the same sample. Changes are expressed relative to the *hspa8*-normalized PD of the E15 sample: [*id* band PD/*hspa8* band PD]/[*id* band PD (E15)/*hspa8* band PD (E15)]. Data reflect the mean normalized fold-change versus E15 ± S.D. (n = 6). *$P < 0.05$. #, phospho-Smad signal was absent; therefore, no ratio could be calculated. Pseud., pseudoglandular; can., canalicular.

2003), as do more recent observations that BMP ligands and Bmpr2 control vasculogenesis (Jeffery et al., 2005b). Our data also hint at a previously unrecognized role for BMP signaling in the homeostasis of the airway epithelium in the developed lung.

EXPERIMENTAL PROCEDURES

Animals and Tissue Treatment

The animal ethics authority of the government of the State of Hessen approved all animal procedures. C57BL/6J mice were housed in humidity- and temperature-controlled rooms on a 12:12-hr light-dark cycle and were allowed food and water ad libitum. Mice at stages E15, E17, E19, P1, P3, P5, P7, P14, P21, and P28 were sacrificed by intraperitoneal injection of sodium pentobarbital. Lungs were excised, flushed free of blood with PBS, and processed immediately for RNA or protein extraction. For histology, the heart and lungs from mice at days P7 and P28 were excised en bloc, and the lungs were pressure fixed overnight at 20 cm H_2O with 4% (m/v) paraformaldehyde in phosphate-buffered saline (PBS; 20 mM Tris-Cl, 137 mM NaCl, pH 7.6), as described previously (Yildirim et al., 2006). Paraffin sections (3 μm) were mounted on poly-L-lysine-coated glass slides, dewaxed with xylene (3 × 5 min) and rehydrated in a graduated series of ethanol solutions (100% (v/v), 95% (v/v), 70% (v/v), and finally PBS).

RNA Isolation and Semi-Quantitative RT-PCR

Total RNA was isolated from fresh lung tissue using a Qiagen RNeasy kit (Qiagen, Hilden, Germany). One microgram of total RNA was reverse-transcribed using the ImProm-II Reverse Transcription System (Promega, Mannheim, Germany). One microliter of the RT reaction served as a template in a PCR reaction using Platinum *Taq* (Invitrogen, Karlsruhe, Germany). Total RNA was screened by semi-quantitative reverse transcription (RT) polymerase chain reaction (PCR) using the following intron-spanning forward (for) and reverse (rev) primers: *bmpr1a* (30 cycles): 5′-GCC TCC CTC ATT CAC TTA CAC-3′ (for), 5′-CTG CCA TCA AAG AAC GGA C-3′ (rev); *bmpr1b* (30 cycles): 5′-CCG GAA GAC TCA GTC AAC AAT-3′ (for), 5′-GAG GAG TAG GCT AGC TTC AGC-3′ (rev); *bmpr2* (31 cycles): 5′-GGG GAA GAA GAT AAT GCG-3′ (for), 5′-GG ACA TCG AAT GCT CAG AGG-3′ (rev); *gapdh* (24 cycles): 5′-GAG AAT GGG AAG CTG GTC AT-3′ (for), 5′-GAA GAC GCC AGT AGA CTC CA-3′ (rev); *hspa8* (25 cycles): 5′-CAA GCG AAA GCA CAA GAA AGA CAT-3′ (for), 5′-ATA CCA AGC GAA AGA GGA GTG ACA TC-3′ (rev); *id1* (19 cycles): 5′-GCC CCA GAA CCG CAA AGT GA-3′ (for), 5′-AAC CCC CTC CCC AAA GTC TCT G-3′ (rev); *id2* (19 cycles): 5′-AAA GCC TTC AGT CCG GTG AG-3′ (for), 5′-AGC CAC AGA GTA CTT TGC TAT CAT-3′ (rev); *id3* (29 cycles): 5′-CGC GAG GCC GCG GTA AG-3′ (for), 5′-GCC AGG GTT GCA CTA AAC AT-3′ (rev); *smad1* (27 cycles): 5′-CTC CTT GGG TGG AAA CAG GG-3′ (for), 5′-TCA TTT TGT CCC AGG TTG CA-3′ (rev); *smad4* (26 cycles) 5′-ACA GAG AAC ATT GGA TGG AC-3′ (for), 5′-AGT AGC TGG CTG AGC AGT AA-3′ (rev); *smad5* (32 cycles) 5′-AGG TGA CGA GGA AGA GA-3′ (for), 5′-GGC TGT TAG GAG ATA AGG-3′ (rev); *smad8* (33 cycles): 5′-GAG CAC CCC CAT CTT CGT CAA-3′ (for) 5′-AAC AGG GGC AGG AGG TGA TG-3′ (rev). Amplicons were separated on a 1% (m/v) agarose gel and visualized by ethidium bromide staining. Amplicons generated with these primer pairs were validated by sequencing, and the stated cycle numbers lie in the logarithmic phase for each PCR. Tissue was not pooled, and individual amplicons are derived from RNA extracted from a single lung. Amplicons are illustrated for two different mouse lungs per developmental stage, which are representative of trends observed in at least six other mouse lungs at the same stage. Amplicons derived from six different mouse lungs per developmental stage were selected for densitometric analysis. For quantification of changes in mRNA expression, band intensities from specific samples were normalized for loading using the constitutively-expressed *hspa8* band from the same sample. Densitometric analysis of amplicon bands was performed using a GS-800 model calibrated densitometer with Quantity One software (both from Bio-Rad Laboratories, Munich, Germany). Changes are expressed relative to the *hspa8*-normalized pixel density (PD) of the E15 sample: [band PD/*hspa8* PD]/[band PD (E15)/*hspa8* PD (E15)].

Additional forward (F) and reverse (R) primers were employed to determine *bmpr1a* splice-isoform expression in the mouse lung: F1: 5′-CCA GTT GAG ACA GCA GGA CC-3′; F2: 5′-CCA TCC TAT GAG GAC ATG CGT G-3′; R1: 5′-GGT GAG CAC AGA GTA ACT CG-3′; R2: 5′-AGT CTG GAG GCT GGA TTA TGG G-3′; R3: 5′-TCA AAT CTT TAC ATC CTG GG-3′; R4: 5′-GTC TAA ATT CTC CCT CAA AA-3′. The approximate location of these primers on the *bmpr1a* mRNA is illustrated in Figure 2. Amplicons generated with these primer pairs were validated by sequencing.

Protein Isolation and Immunoblotting

Protein extraction from mouse lungs, gel electrophoresis, and immunoblotting were performed as described previously (Alejandre-Alcázar et al., 2007). Mouse lung protein extracts (10 μg) were resolved on 12% polyacrylamide gels and transferred to nitrocellulose membranes for immunoblotting. Blots were probed with: rabbit anti-Smad1 (1:1,000; Cell Signaling Technology, Danvers, MA), rabbit anti-Smad5 (1:1,000; Zymed, San Francisco, CA), goat anti-Smad8 (1:750; R&D Systems, Wiesbaden, Germany), rabbit anti-phospho-Smad1/5(Ser463/ser465) (1:1,000; Cell Signaling, Danvers, MA), and anti-Smad4 (1:1,000; Upstate, Charlottesville, VA). The generation of rabbit polyclonal anti-peptide antibodies (used at 1:1,000) against Bmpr1a, Bmpr1b, and Bmpr2 has been described previously (Gilboa et al., 2000). Rabbit anti-α-tubulin (Cell Signaling Technology, Danvers, MA; 1:1,000) served as a loading control. Peroxidase-conjugated secondary antibodies were from R&D Systems (1:2,500; Wiesbaden, Germany). Tissue was not pooled, and individual bands on immunoblots are derived from a single lung. Blots illustrate samples from two different mouse lungs per developmental stage, which are representative of trends observed in at least six other mouse lungs at the same stage. Bands derived from six different mouse lungs per developmental stage were selected for densitometric analysis. Band intensities from samples were normalized for loading using the α-tubulin band from the same sample. Expression ratios for immunoblot data reflect values normalized for tubulin: [band PD/tubulin band PD]/[band PD (E15)/tubulin band PD (E15)].

Immunohistochemistry

Hematoxylin staining, and expression of BMP receptors, Smads, and smooth muscle actin (SMA) was assessed on 3-μm tissue sections as described previously (Morty et al., 2007), with anti-SMA (1:850; clone 1A4; Sigma, Taufkirchen, Germany); rabbit anti-Bmpr1a (1:150), -Bmpr1b (1:150) and -Bmpr2 (1:150) (Gilboa et al., 2000); and rabbit anti-Smad1, -Smad4, and -Smad5 (all at 1:50; Zymed, San Fransisco, CA) and goat anti-Smad8 ((1:50; R&D Systems, Wiesbaden, Germany). Immune-complexes were visualized with a Histostain *Plus* Kit (Zymed, San Fransisco, CA). The specificity of all antibodies employed for immunohistochemistry has been validated (Gilboa et al., 2000; Alejandre-Alcázar et al., 2007; Morty et al., 2007; Zakrzewicz et al., 2007).

Statistical Treatment of Data

Data are presented as mean ± S.D. Differences between groups were analyzed by ANOVA and the Student-Newman-Keul post-hoc test for multiple comparisons, with $P < 0.05$ regarded as significant.

REFERENCES

Alejandre-Alcázar MA, Kwapiszewska G, Reiss I, Amarie OV, Marsh LM, Sevilla-Pérez J, Wygrecka M, Eul B, Kobrich S, Hesse M, Schermuly RT, Seeger W, Eickelberg O, Morty RE. 2007. Hyperoxia modulates TGF-beta/BMP signaling in a mouse model of bronchopulmonary dysplasia. Am J Physiol Lung Cell Mol Physiol 292:L537–549.

Bellusci S, Henderson R, Winnier G, Oikawa T, Hogan BL. 1996. Evidence from normal expression and targeted misexpression that bone morphogenetic protein (Bmp-4) plays a role in mouse embryonic lung morphogenesis. Development 122:1693–1702.

Bragg AD, Moses HL, Serra R. 2001. Signaling to the epithelium is not sufficient to mediate all of the effects of transforming growth factor beta and bone morphogenetic protein 4 on murine embryonic lung development. Mech Dev 109:13–26.

Buckley S, Shi W, Driscoll B, Ferrario A, Anderson K, Warburton D. 2004. BMP4 signaling induces senescence and modulates the oncogenic phenotype of A549 lung adenocarcinoma cells. Am J Physiol Lung Cell Mol Physiol 286:L81–86.

Cardoso WV. 2001. Molecular regulation of lung development. Annu Rev Physiol 63: 471–494.

Chen C, Chen H, Sun J, Bringas P Jr, Chen Y, Warburton D, Shi W. 2005. Smad1 expression and function during mouse embryonic lung branching morphogenesis. Am J Physiol Lung Cell Mol Physiol 288:L1033–1039.

Copland I, Post M. 2004. Lung development and fetal lung growth. Paediatr Respir Rev 5 Suppl A:S259–264.

de Caestecker M. 2004. The transforming growth factor-beta superfamily of receptors. Cytokine Growth Factor Rev 15:1–11.

Dewulf N, Verschueren K, Lonnoy O, Moren A, Grimsby S, Vande Spiegle K, Miyazono K, Huylebroeck D, Ten Dijke P. 1995. Distinct spatial and temporal expression patterns of two type I receptors for bone morphogenetic proteins during mouse embryogenesis. Endocrinology 136:2652–2663.

Du L, Sullivan CC, Chu D, Cho AJ, Kido M, Wolf PL, Yuan JX, Deutsch R, Jamieson SW, Thistlethwaite PA. 2003. Signaling molecules in nonfamilial pulmonary hypertension. N Engl J Med 348:500–509.

Eblaghie MC, Reedy M, Oliver T, Mishina Y, Hogan BL. 2006. Evidence that autocrine signaling through Bmpr1a regulates the proliferation, survival and morphogenetic behavior of distal lung epithelial cells. Dev Biol 291:67–82.

Frank DB, Abtahi A, Yamaguchi DJ, Manning S, Shyr Y, Pozzi A, Baldwin HS, Johnson JE, de Caestecker MP. 2005. Bone morphogenetic protein 4 promotes pulmonary vascular remodeling in hypoxic pulmonary hypertension. Circ Res 97:496–504.

Gilboa L, Nohe A, Geissendorfer T, Sebald W, Henis YI, Knaus P. 2000. Bone morphogenetic protein receptor complexes on the surface of live cells: a new oligomerization mode for serine/threonine kinase receptors. Mol Biol Cell 11:1023–1035.

Hassel S, Schmitt S, Hartung A, Roth M, Nohe A, Petersen N, Ehrlich M, Henis YI, Sebald W, Knaus P. 2003. Initiation of Smad-dependent and Smad-independent signaling via distinct BMP-receptor complexes. J Bone Joint Surg Am (85-A Suppl) 3:44–51.

Izumi N, Mizuguchi S, Inagaki Y, Saika S, Kawada N, Nakajima Y, Inoue K, Suehiro S, Friedman SL, Ikeda K. 2006. BMP-7 opposes TGF-beta1-mediated collagen induction in mouse pulmonary myofibroblasts through Id2. Am J Physiol Lung Cell Mol Physiol 290:L120–126.

Jankov RP, Tanswell AK. 2004. Growth factors, postnatal lung growth and bronchopulmonary dysplasia. Paediatr Respir Rev 5 Suppl A:S265–275.

Jeffery TK, Upton PD, Trembath RC, Morrell NW. 2005a. BMP4 inhibits proliferation and promotes myocyte differentiation of lung fibroblasts via Smad1 and JNK pathways. Am J Physiol Lung Cell Mol Physiol 288:L370–378.

Jeffery TK, Upton PD, Yang X, Southwood M, Long L, Trembath RC, Morrell NW. 2005b. Does BMPR2 mutation disrupt pulmonary vasculogenesis? Chest 128:602S.

Koenig BB, Cook JS, Wolsing DH, Ting J, Tiesman JP, Correa PE, Olson CA, Pecquet AL, Ventura F, Grant RA, et al. 1994. Characterization and cloning of a receptor for BMP-2 and BMP-4 from NIH 3T3 cells. Mol Cell Biol 14:5961–5974.

Lu MM, Yang H, Zhang L, Shu W, Blair DG, Morrisey EE. 2001. The bone morphogenic protein antagonist gremlin regulates proximal-distal patterning of the lung. Dev Dyn 222:667–680.

Miyazono K, Miyazawa K. 2002. Id: a target of BMP signaling. Sci STKE DOI: 10.1126/stke.2002.151.pe40.

Miyazono K, Maeda S, Imamura T. 2005. BMP receptor signaling: transcriptional targets, regulation of signals, and signaling cross-talk. Cytokine Growth Factor Rev 16:251–263.

Morty RE, Nejman B, Kwapiszewska G, Hecker M, Zakrzewicz A, Kouri FM, Peters DM, Dumitrascu R, Seeger W, Knaus P, Schermuly RT, Eickelberg O. 2007. Dysregulated bone morphogenetic protein signaling in monocrotaline-induced pulmonary arterial hypertension. Arterioscler Thromb Vasc Biol 27:1072–1078.

Panchision DM, Pickel JM, Studer L, Lee SH, Turner PA, Hazel TG, McKay RD. 2001. Sequential actions of BMP receptors control neural precursor cell production and fate. Genes Dev 15:2094–2110.

Rosendahl A, Pardali E, Speletas M, Ten Dijke P, Heldin CH, Sideras P. 2002. Activation of bone morphogenetic protein/Smad signaling in bronchial epithelial cells during airway inflammation. Am J Respir Cell Mol Biol 27:160–169.

Roth-Kleiner M, Post M. 2003. Genetic control of lung development. Biol Neonate 84:83–88.

Roth-Kleiner M, Post M. 2005. Similarities and dissimilarities of branching and septation during lung development. Pediatr Pulmonol 40:113–134.

Shi W, Zhao J, Anderson KD, Warburton D. 2001. Gremlin negatively modulates BMP-4 induction of embryonic mouse lung branching morphogenesis. Am J Physiol Lung Cell Mol Physiol 280:L1030–1039.

Shi W, Chen H, Sun J, Chen C, Zhao J, Wang YL, Anderson KD, Warburton D.

2004. Overexpression of Smurf1 negatively regulates mouse embryonic lung branching morphogenesis by specifically reducing Smad1 and Smad5 proteins. Am J Physiol Lung Cell Mol Physiol 286: L293–300.

Trembath RC, Thomson JR, Machado RD, Morgan NV, Atkinson C, Winship I, Simonneau G, Galie N, Loyd JE, Humbert M, Nichols WC, Morrell NW, Berg J, Manes A, McGaughran J, Pauciulo M, Wheeler L. 2001. Clinical and molecular genetic features of pulmonary hypertension in patients with hereditary hemorrhagic telangiectasia. N Engl J Med 345: 325–334.

Wall NA, Blessing M, Wright CV, Hogan BL. 1993. Biosynthesis and in vivo localization of the decapentaplegic-Vg-related protein, DVR-6 (bone morphogenetic protein-6). J Cell Biol 120:493–502.

Warburton D, Schwarz M, Tefft D, Flores-Delgado G, Anderson KD, Cardoso WV. 2000. The molecular basis of lung morphogenesis. Mech Dev 92:55-81.

Warburton D, Bellusci S, De Langhe S, Del Moral PM, Fleury V, Mailleux A, Tefft D, Unbekandt M, Wang K, Shi W. 2005. Molecular mechanisms of early lung specification and branching morphogenesis. Pediatr Res 57:26R–37R.

Weaver M, Yingling JM, Dunn NR, Bellusci S, Hogan BL. 1999. Bmp signaling regulates proximal-distal differentiation of endoderm in mouse lung development. Development 126:4005–4015.

Yang X, Lee PJ, Long L, Trembath RC, Morrell NW. 2007. BMP4 induces HO-1 via a Smad independent, p38^{MAPK} dependent pathway in pulmonary artery myocytes. Am J Respir Cell Mol Biol (in press).

Yildirim AO, Bulau P, Zakrzewicz D, Kitowska KE, Weissmann N, Grimminger F, Morty RE, Eickelberg O. 2006. Increased protein arginine methylation in chronic hypoxia: role of protein arginine methyltransferases. Am J Respir Cell Mol Biol 35:436–443.

Yu PB, Beppu H, Kawai N, Li E, Bloch KD. 2005. Bone morphogenetic protein (BMP) type II receptor deletion reveals BMP ligand-specific gain of signaling in pulmonary artery smooth muscle cells. J Biol Chem 280:24443–24450.

Zakrzewicz A, Kouri FM, Nejman B, Kwapiszewska G, Hecker M, Sandu R, Dony E, Seeger W, Schermuly RT, Eickelberg O, Morty RE. 2007. The transforming growth factor-beta/Smad2,3 signalling axis is impaired in experimental pulmonary hypertension. Eur Respir J 29:1094–1104.